Building and Environment 265 (2024) 111911

Contents lists available at ScienceDirect

Building and Environment

journal homepage: www.elsevier.com/locate/buildenv

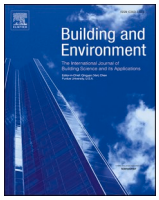

Infection-prevention performance of local exhaust ventilation under three different underfloor air distribution systems during a face-to-face conversation

Jun Yoshihara [a,*], Toshio Yamanaka [a], Narae Choi [b], Tomohiro Kobayashi [a], Noriaki Kobayashi [a], Aoi Fujiwara [a]

[a] Department of Architectural Engineering, Graduate School of Engineering, Osaka University, 2-1 Yamadaoka, Suita, Osaka, 565-0871, Japan
[b] Department of Architecture, Faculty of Science and Engineering, Toyo University, 5 Chome-28-20 Hakusan, Tokyo, Japan

ARTICLE INFO

Keywords:
Floor-supply displacement ventilation (FSDV)
Local exhaust ventilation (LEV)
Consulting (examination) room
SARS-CoV-2
Airborne transmission
Wells-Riley model

ABSTRACT

This study proposes using a local exhaust ventilation system (LEV) to prevent airborne infections, especially for short-range conversations. We compared the performance of a hood in three different underfloor air distribution systems (UFAD): floor-supply displacement ventilation (FSDV), horizontal flow-type floor diffuser (HFD), and swirling flow-type floor diffuser (SFD). Two situations were considered: Case A, a consulting room, and Case B, a restaurant or meeting room. The difference in infection risk assessment between using CO_2 and artificial saliva particles as tracers of exhaled breath was also discussed. Results indicate that the distribution of exhaled air and infection risk for doctors decreased in the order FSDV < HFD < SFD. Although the effect of introducing hoods was confirmed to a certain degree for the three ventilation methods in Case A, the effect of the hoods on the quanta concentration of the facing person was small in Case B. Comparing airborne infection risks between gas and particles, particle-based airborne infection was smaller in the FSDV due to the more significant impact of particle adhesion and falling. As a limitation, the ventilation rate in the experiment was 1000 m^3/h (50 ACH). Therefore, the air supply method had a more significant impact on the results than the hood method. A practical implication of this experiment is that even under high ventilation volumes (50 ACH), the FSDV can reduce the horizontal distribution of the patient's exhaled air and prevent airborne infection. These results should be adapted to smaller spaces such as examination rooms and meeting rooms.

1. Introduction

Since 2019, the SARS-CoV-2 (COVID-19) pandemic has drastically affected the global population. According to the World Health Organization (WHO) COVID-19 dashboard, over 774 million cases have been confirmed globally as of March 17, 2024 [1]. More than 292,000 new cases and 6200 new deaths were reported to the WHO during a 28-day period (February 5 to March 3, 2024) [2]. These situations have attracted increased attention to ventilation as an infection control measure [3,4]. Regarding its transmission modes, the possibility of airborne transmission was discussed widely in the early stages of the pandemic [5–8]. With the contributions of many studies that showed evidence of airborne transmission in past outbreak events [9–11], airborne transmission has been widely recognized as one of the main modes of transmission for COVID-19 [12–14]. Ventilation is an effective method for diluting the concentration of infectious contaminants in a room [15]. The Federation of European Heating Ventilation and Air Conditioning Associations (RHEVA) has published guidance for COVID-19, discussing the relationship between ventilation rate and infection risk under the assumption of perfect mixing [16]. However, REHVA also mentioned that room-scale ventilation might not be sufficient to entirely prevent infections in close contact scenarios (within 1–2m) [16]. In many scenarios, such as in hospital consulting (examination) rooms, restaurants, or crowded trains, short-distance conversations are unavoidable. Therefore, this study proposes the use of local exhaust ventilation systems (LEV), which are mainly used in factories and kitchens, for managing short-distance conversations (Fig. 1.). LEVs, commonly known as hoods, have been developed for factories and kitchens to capture contaminants harmful to human health and to maintain safe breathing zones for workers [17–19]. Many studies have investigated the relationship between hood flow rate, pollution source

* Corresponding author.
E-mail address: yoshihara_jun@arch.eng.osaka-u.ac.jp (J. Yoshihara).

https://doi.org/10.1016/j.buildenv.2024.111911
Received 24 May 2024; Received in revised form 26 July 2024; Accepted 31 July 2024
Available online 8 August 2024

Nomenclature

Acronyms

LEV	local exhaust ventilation system
UFAD	underfloor air distribution systems
FSDV	floor-supply displacement ventilation
HFD	horizontal flow-type floor diffuser
SFD	swirling flow-type floor diffuser
OTV	occupant targeted ventilation Conditioning
WHO	World Health Organization
REHVA	Federation of European Heating Ventilation and Air Conditioning Associations
HEPA	High Efficiency Particulate Air Filter
EDIS	Expiratory Droplet Investigation System

Symbols

C_{ni}	particle number concentration for each interval [m^{-3}]
D_i	arithmetic interval width [m]
n_i	measured number of particles within the interval borders $D_{i,\ upper}$ and $D_{i,\ lower}$ [p]
V_m	measured volume [m^3]
$D_{i,upper}$	the diameter of the upper interval border [m]
$D_{i,lower}$	the diameter of the lower interval border [m]
Q_h	hood exhaust flow rate [m^3/h]
C_h	tracer gas (CO_2) concentration of hood exhaust air [−]
C_{SA}	tracer gas (CO_2) constatation of supply air [−]
Q_e	ceiling exhaust flow rate [m^3/h]
C_e	tracer gas (CO_2) concentration of ceiling exhaust air [−]
P	increased rate of the number of newly infected persons in a closed space [−]
n	value of the quanta [quanta]
C_{qd}	quanta concentration in front of the doctor's (non-infected person's) mouth [quanta/m^3]
q	quanta emission rate [quanta/h]
Q	room ventilation rate [m^3/h]
C_{dg}	tracer gas concentration in front of the doctor's mouth [−]
M_g	tracer gas (CO_2) emission rate [m^3/h]
C_{nd}	CO_2 normalized concentration in front of the doctor's mouth [−]
Q_{pt}	the volume flow rate of particle counter [m^3/h] (=2.81 L/min)
V_{dp}	the total volume of particles in front of the doctor's mouth measured by particle counter divided by measurement time (15 min) [m^3/h]
V_{ep}	the total generated volume of particles divided by emission time (20 min) [m^3/h]
M_{ab}	mass of artificial saliva before emission [g]
M_{aa}	the mass of artificial saliva after emission [g]
R_c	compositional ratios of artificial saliva after evaporation to before evaporation [−]
ρ_{aa}	density of artificial saliva after evaporation [g/m^3] (=1.09 g/m^3)
ρ_{ab}	the density of artificial saliva before evaporation [g/m^3]
R_d	diameter ratio of particles after evaporation to before evaporation [−]
$t_{5\%}$	time until the doctor's (non-infected person) infection risk reaches 5 % [h]

distance, and plume volume to determine hood capture efficiency [20, 21]. Therefore, LEV is expected to effectively capture droplets and droplet nuclei emitted from the mouth with a certain velocity. Ventilation focused on the breathing zone can be considered a type of personal ventilation (PV) [22]. This study can be regarded as an examination of the personal exhaust. While several studies have evaluated and demonstrated PV's effectiveness as an airborne infection control measure, they have not focused sufficiently on the spread of contaminants [23–25]. However, to reduce the risk of infection in an entire room, it is ideal to capture and exhaust contaminants without spreading them. In

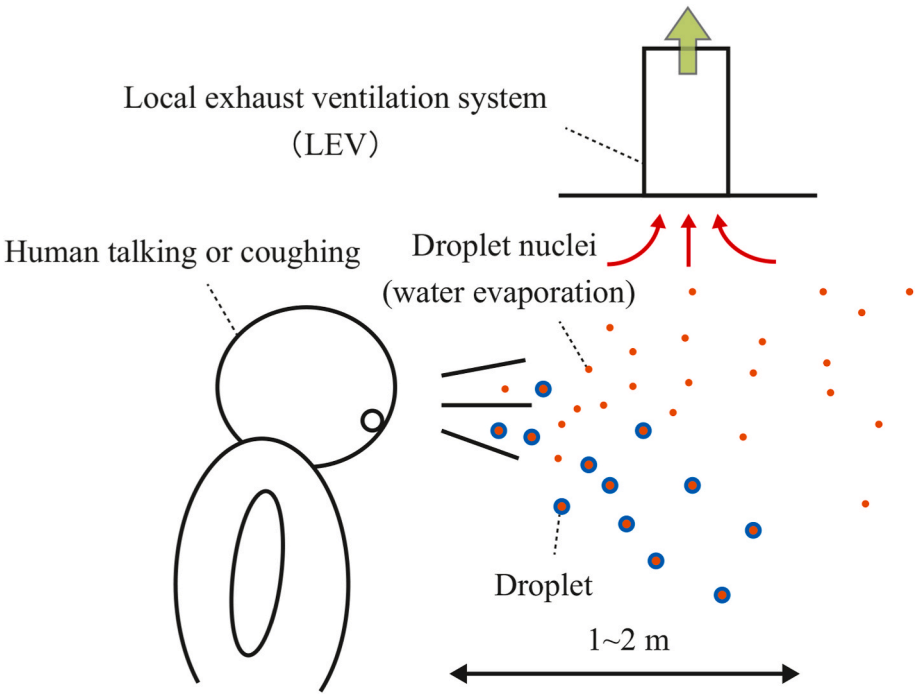

Fig. 1. Concepts of the research.

addition, exhausting most of the infectious contaminants through LEV ensures that the returned air is safe through other exhaust routes in HVAC systems. Therefore, the authors believe that LEV installation aims to capture contaminants as completely as possible without spreading them. On the other hand, Melikov et al. defined Occupant Targeted Ventilation (OTV) as ventilation that prioritizes health and comfort for individual and group occupants and non-uniform air distribution [26]. From this perspective, PV is a type of OTV, and the system in this study can also be considered a type of OTV.

Komori et al. showed that the capture performance of hoods is significantly affected by the passing airflow [27], and a calm airflow field is required to understand a hood's fundamental performance. However, in practice, indoor airflow is often large and turbulent. This study compares three types of underfloor air distribution methods (UFAD) to clarify the relationship between the surrounding airflow and hood capture performance. The first type is floor-supply displacement ventilation (FSDV) (Fig. 2. (a-1) and (b-1)), in which air is supplied from an underfloor chamber through an air-permeable carpet. FSDV was mainly developed by Olesen et al. and Akimoto et al., in 1993 as a type of displacement ventilation (DV) [28,29]. In FSDV, air is supplied from a larger area, making the mean air velocity of the entire room quite small. Lau and Chen showed that FSDV is superior to swirl diffusers as an airborne infection control measure [30]. In this study, FSDV is expected to represent the hood's most basic performance. The second type is a horizontal flow-type floor diffuser (HFD) (Fig. 2. (a-2) and (b-2)), expected to form displacement ventilation by blowing horizontally. Displacement ventilation (DV) forms a vertical temperature gradient by supplying relatively calm airflow from the floor or wall below. In an appropriate DV airflow field, heat source contaminants can be exhausted without stagnating in the breathing zone [31,32]. HFD is expected to form a relatively quiet airflow field, although not as quiet as an FSDV. The third type is a swirling flow-type floor diffuser (SFD) (Fig. 2. (a-3) and (b-3)), which distributes air throughout the room via swirling flow. SFD is often used in practical facility designs because of its ability to distribute fresh air widely [33]. However, it is considered unsuitable as an infection control measure because it promotes room-air mixing [30]. SFD experiments will be conducted for comparison, although it is expected to have a negative effect on the hood's capture performance.

Considering this situation, the consulting (examination) room in a hospital was assumed for the following three reasons (Fig. 2. (a-1–3)). First, the hood capture performance is largely affected by the distance from the pollution source [20,34]. Thus, the hood is expected to be effective in consulting rooms where pollution sources are identified. Second, there is a high risk of conversation between infected and uninfected persons (e.g., doctors) in a consulting room. Third, ventilation for infection control in consulting rooms and hospitals, where doctors may talk to various infected patients, will remain in demand, even after the COVID-19 pandemic has settled. It is also possible to have a short-distance conversation with an infected person, except in a consultation room, and there have been many cases of airborne infections in restaurants [11]. Therefore, to investigate the possibility of applying the hood to restaurants or conference rooms where the location of infectors cannot be identified, we will conduct an experiment in which the hood is placed between humans and a desk (Fig. 2. (b-1–3)).

In a previous study by the authors, CFD analysis demonstrated the significant impact of introducing hoods on close-range conversations under 6ACH conditions [34]. However, the previous study was limited to a CFD trial, and actual experiments are required to verify the results [34]. This paper presents laboratory experiments to examine the effectiveness of hood introduction and the effect of ambient airflow on hood capture performance. Regarding the reproducibility of human-derived droplets and droplet nuclei, previous studies often employed tracer gases (N_2O, CO_2) to simulate the spread of droplet nuclei [35–37]. According to the World Health Organization (WHO), droplets evaporate after release from the mouth and become droplet nuclei (<5 μm) that drift in the air [38]. Because droplet nuclei are passive contaminants that move with the air, airflow control is considered an effective measure against airborne infections. Therefore, simulating droplet nuclei with tracer gas is often used to study airborne infections. However, the behavior of droplets is different from that of actual human-derived

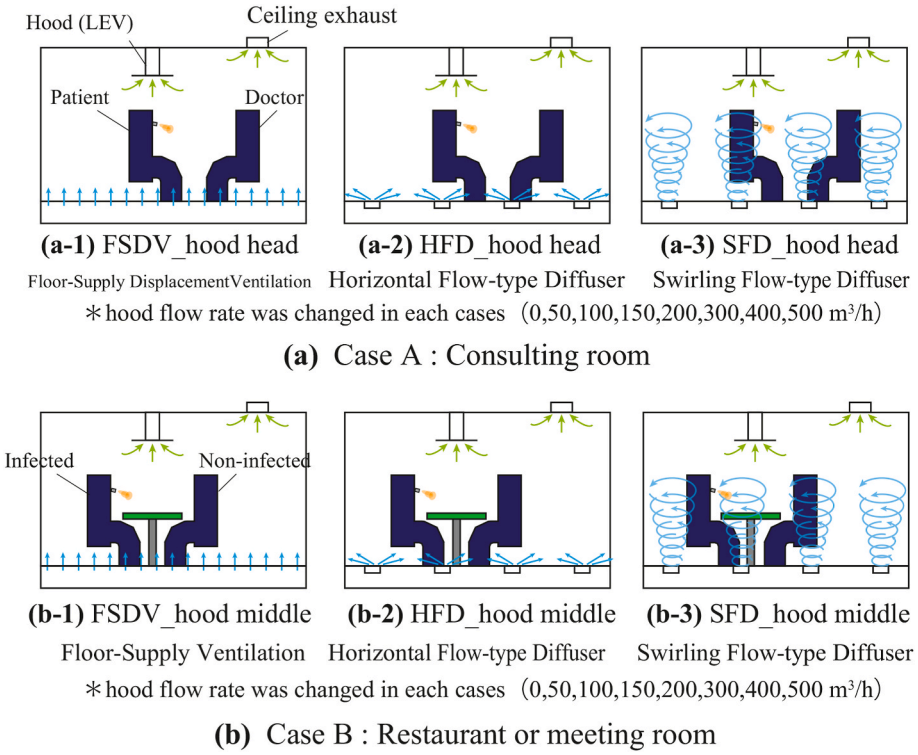

Fig. 2. Conceptual drawing of experimental parameters. (a) Case A: consulting room. (a-1) FSDV_hood head. (a-2) HFD_hood head. (a-3) SFD_hood head. (b) Case B: restaurant or meeting room. (b-1) FSDV_ hood middle. (b-2) HFD_hood middle. (b-3) SFD_hood middle.

particles because of the effects of adhesion and falling. Considering this effect, this experiment aims to investigate how variations in gas and particle behavior influence infection risk assessment by simultaneously emitting artificial saliva particles using a nebulizer and releasing tracer gas.

The objectives and outline of this study are as follows.

- Evaluate the effectiveness of hoods as an infection control measure for short-distance conversations through a full-scale experiment.
- Examine the impact of differences in tracer gas (CO_2+He) and particle behavior on infection risk assessment.
- Compare three different underfloor air distribution systems to evaluate the impact of surrounding airflow on hood capture performance.
- Position the hood above the patient's head in consulting room conditions, where the location of the pollution source and infectors are easy to identify.
- Position the hood between individuals with a desk in settings where identifying the pollution source and infectors, such as restaurants or meeting rooms, is challenging.

Note that in this paper, the ventilation rate is fixed at 1000 m^3/h (50 ACH), limited by the laboratory equipment. The authors acknowledge that this value is considerably larger than the 6–12 ACH (REHVA, WHO) required in the design process [15,16]. Therefore, this study aims to understand the performance of hoods under high ventilation rates, where the surrounding airflow is highly turbulent. Further study is required to examine the actual situation of hood introductions. In addition, this study considers droplets and droplet nuclei generated during conversations, which are expected to have a hood introduction effect, but does not consider coughs with greater momentum. Regarding the velocity of droplet generation in this study, the data on the velocity of breathing without masking, which was measured in the previous study, was given to reproduce conversation [34].

2. Experimental method and materials

2.1. Experimental cases and facilities

A cross-sectional view of the experimental room is shown in Fig. 3 (a), and an isometric view is shown in Fig. 3 (b). The experimental room measured x = 2,400, y = 3,800, and z = 2200 mm and included an underfloor chamber, where outside air, cleaned using a HEPA filter, was supplied. The air supply rate was fixed at 1000 m^3/h (50 ACH) due to the power of the outside air conditioner. This high ventilation rate causes frictional noise as the air passes through the ducts, although not enough to disturb the stress-free conversations in the room. The total flow rate of exhaust air was 990 m^3/h through the local exhaust ventilation system (hood) and general ceiling exhaust, and the room was designed as a clean room to maintain positive pressure. In addition, two human bodies, simulating an infected person and a non-infected person (each generating 75 W of heat), were placed in the room at intervals of a mouth-to-mouth distance of 1200 mm. A flanged hood was used because it had the best capture performance under a crosswind airflow in a previous study (Fig. 3 (c)) [27]. The experimental cases are summarized in Table 1. The experimental cases were divided into Case A, consulting room, and Case B, restaurant or meeting room, as described in the introduction, with the conceptual diagram shown in Fig. 2. In Case A, the hood was placed above the patient's head in a hospital consulting room, and in Case B, the hood was placed in the middle of a mannequin in a restaurant or conference room because it was unknown which of the two was infected. A desk was also placed between the humans. The relationship between the distance between the hood and the emission source is shown in Fig. 3 (c). As shown in Figs. 3 (c-1), hood introduction was expected to be more effective in Case A, where the distance between the emission source and the hood was smaller. In each case, the underfloor air supply system was tested in three patterns: floor-supply displacement ventilation (FSDV), horizontal flow-type floor diffuser (HFD), and swirling flow-type floor diffuser (SFD). According to the manufacturer's catalog, the airflow spread angle for HFDs is about 10–15° from the floor, and for SFDs about ±10–15° from the vertical. The details of each floor distribution system are shown in Fig. 4. In the FSDV, air was supplied from the entire floor through a permeable carpet, while air was supplied through several diffusers in the HFD and SFD. The

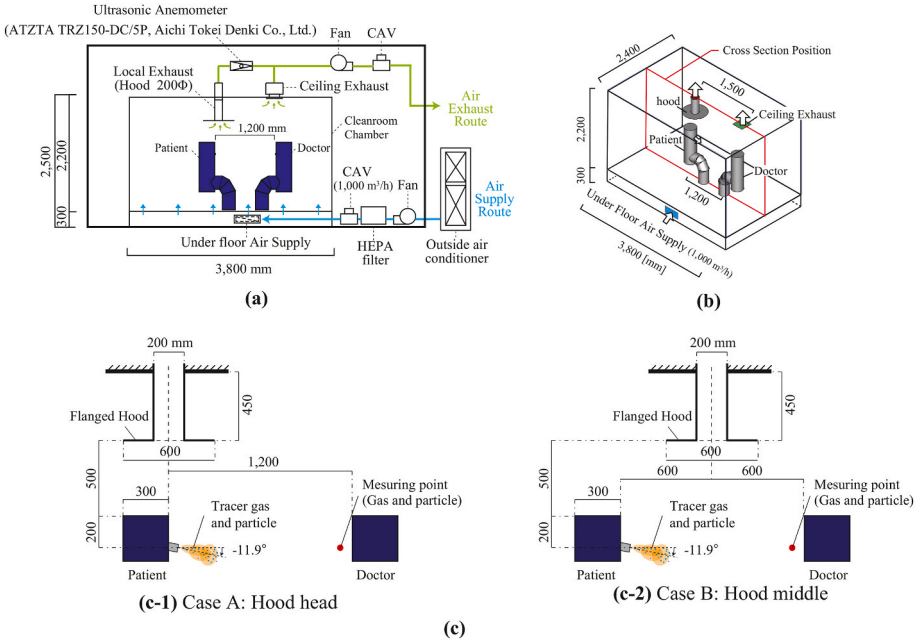

Fig. 3. Full-scale experiment settings. (a) Cross-sections of experimental facilities. (b) Isometric drawing of cleanroom chamber. (c) Relation between emission point and hood location. (c-1) Case A: hood above the patient's head. (c-2) Case B: hood middle of the mannequins.

Table 1
Summarization of experimental cases.

Groupe	Considered situations	Case name	Air supply method	Hood horizontal potistions	Hood exhaust flow rate [m^3/h]
Case A	Consulting room	FSDV_hood head	Floor-supply displacement ventilation	Above the patient's head	0,50,100,150,200,300,400,500
		HFD_hood head	Horizontal flow-type floor diffuser		0,50,100,150,200,300,400,500
		SFD_hood head	Swirling flow-type floor diffuser		0,50,100,150,200,300,400,500
Case B	Restaurant or meeting room	FSDV_hood middle	Floor-supply displacement ventilation	Middle of the mannequins	0,50,100,150,200,300,400,500
		HFD_hood middle	Horizontal flow-type floor diffuser		0,50,100,150,200,300,400,500
		SFD_hood middle	Swirling flow-type floor diffuser		0,50,100,150,200,300,400,500

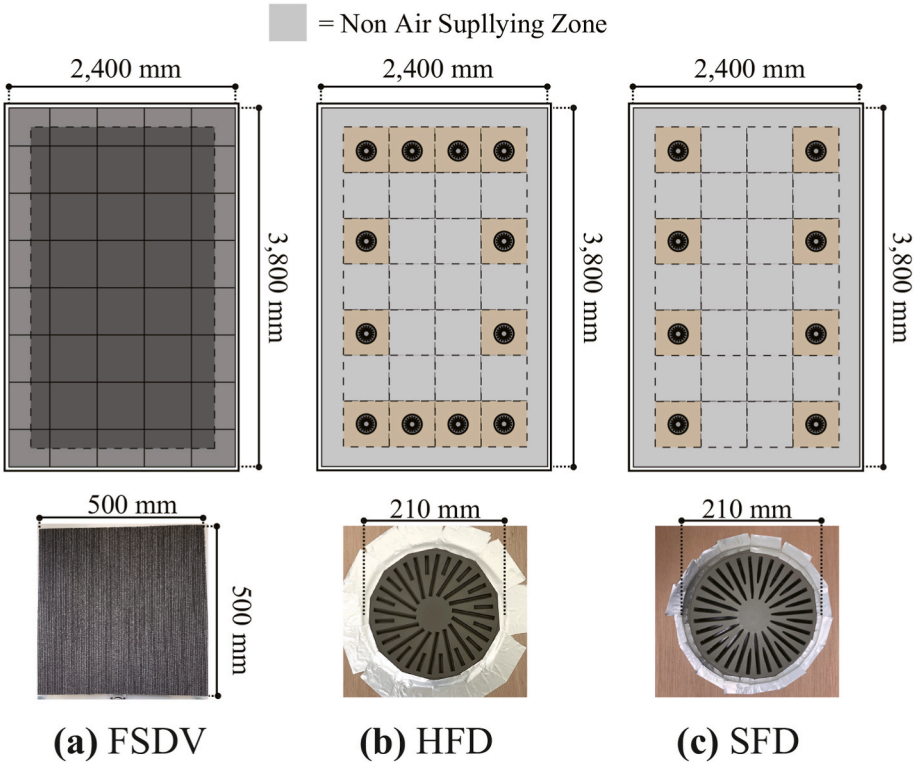

Fig. 4. Floor details of each underfloor air distribution system: (a) FSDV, (b) HFD, and (c) SFD.

air supply volume per diffuser was suitable for the standard flow range indicated by the manufacturer. As mentioned in Section 1, the purpose of the FSDV was to examine the fundamental performance of the hood, and the HFD and SFD were used to examine the effectiveness of the hood when there was turbulence in the surrounding airflow. Additionally, to examine the effect of the hood, its exhaust flow rate was varied as 0, 50, 100, 150, 200, 300, 400, and 500 m^3/h for each floor distribution system. All 48 experimental cases listed in Table 1 were carried out.

2.2. Condition of exhalation generation

The exhaled breath of an infected person was reproduced by simultaneously generating CO_2 tracer gas and artificial saliva particles using a nebulizer. A conceptual diagram of exhalation generation is shown in Fig. 5. CO_2 and Helium gases were mixed at a ratio of 5:3 (CO_2: He = 3.26:1.95 L/min) to equalize the density with that of air and were generated at the height of the infected person's mouth (height: 1100

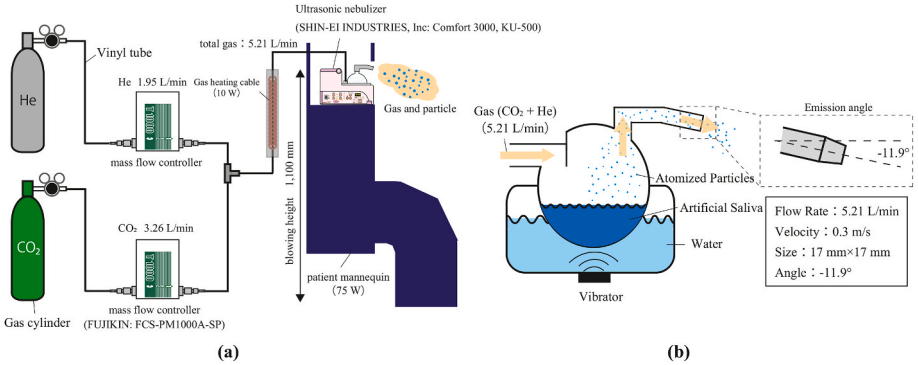

Fig. 5. Tracer gas and particle generation methods. (a) A simultaneous gas and particle generation system. (b) The mechanism of particle generation of the ultrasonic nebulizer.

mm) coupled with atomized artificial saliva. The viscosity of the artificial saliva was adjusted by adding 12 g of sodium chloride and 76 g of glycerin to 1 L of water, as described by Ogata et al. [39]. The atomization method of the ultrasonic nebulizer (SHIN-EI INDUSTRIES, Inc. Comfort 3000 KU-500) is shown in Fig. 5 (b). Particles were produced using a vibrator pushed by the mixed gas and released through the nozzle. The ultrasonic nebulizer was developed for medical use and not for experimental use. Therefore, particle size distribution and number concentration were measured as described in Section 2.3. The exhaled volume, exhaled air velocity, and blow-off angle values during a conversation were obtained from our previous study [34] and were set to 5.21 L/min, 0.30 m/s, and 11.9° vertically downward, respectively. In a previous study, six Asian subjects (3 males, and 3 females, aged 21 to 24, averaging 22.5) read a manuscript in Japanese for 1 min. Velocity and its vector of exhaled air were measured by the ultrasonic anemometer (Sonic corporation: ultrasonic anemometer model DA-700 with TR-92T 30 mm probe), and volume was measured by PET bag and a dry gas meter (SINAGAWA).

2.3. Measurement points and experimental procedures

After the emission, the spatial distributions of the steady-state CO_2 concentration and particle number concentration in front of the doctor's mouth were measured. Fig. 6 shows the details of the measurement points. The CO_2 concentration was measured using six CO_2 recorder (RTR-576, T&D Corporation) units installed on each of the five poles of the Pa–Pe (Fig. 6 (a), (b), and (c)). The CO_2 concentration in front of the doctor's mouth was also measured using a CO_2 recorder, and the particle number concentration was measured using a particle counter (handheld particle counter: model 3888, KANOMAX), as shown in Fig. 6 (c) and (d). These measurements were used to calculate C_{qd}, the quanta concentration in front of the doctor's mouth [quanta/m^3] using Eqs. (5) and (8), as described in Section 2.4.2. Due to the number of instruments, the spatial distribution and concentration in front of the doctor's mouth were measured for CO_2, while only the concentration in front of the doctor's mouth was measured for particles.

Fig. 7 shows the experimental procedure. The decrease in artificial saliva was measured before and after the experiment using an electronic mass balance (GX-8K, A&D Company, Ltd.) to calculate the quanta concentration in front of the doctor's mouth with the particles using Eqs. (5) and (8), as described below (M_{ab}, M_{aa}). The experiment was conducted at 1000 m^3/h (50 ACH). Hence, it took 5 min to reach a steady state. Measurements were taken for 15 min under steady-state conditions, and the average CO_2 and particle number concentrations were used to calculate the hood capture efficiency, CO_2 normalized concentration, and quanta concentration in front of the doctor's mouth, as described in Section 2.4. In all 48 cases, the same time schedule was used for the measurements.

2.4. Assessment criteria

2.4.1. Hood capture performance

The hood capture efficiency, η, which indicates the percentage of the tracer gas captured by the hood, was calculated using Eq. (1).

$$\eta = \frac{Q_h(C_h - C_{SA})}{Q_h(C_h - C_{SA}) + Q_e(C_e - C_{SA})} \quad (1)$$

where Q_h is the hood flow rate [m^3/h], C_h is the tracer gas (CO_2) concentration of hood exhaust air [−], Q_e is the ceiling exhaust flow rate [m^3/h], C_e is the tracer gas (CO_2) concentration of ceiling exhaust air [−], C_{SA} is the tracer gas (CO_2) constatation of supply air [−]. Q_h was measured using an ultrasonic anemometer (ATZTA TRZ150-DC/5P, Aichi Tokei Denki Co., Ltd.), as shown in Fig. 3 (a). The CO_2 gas

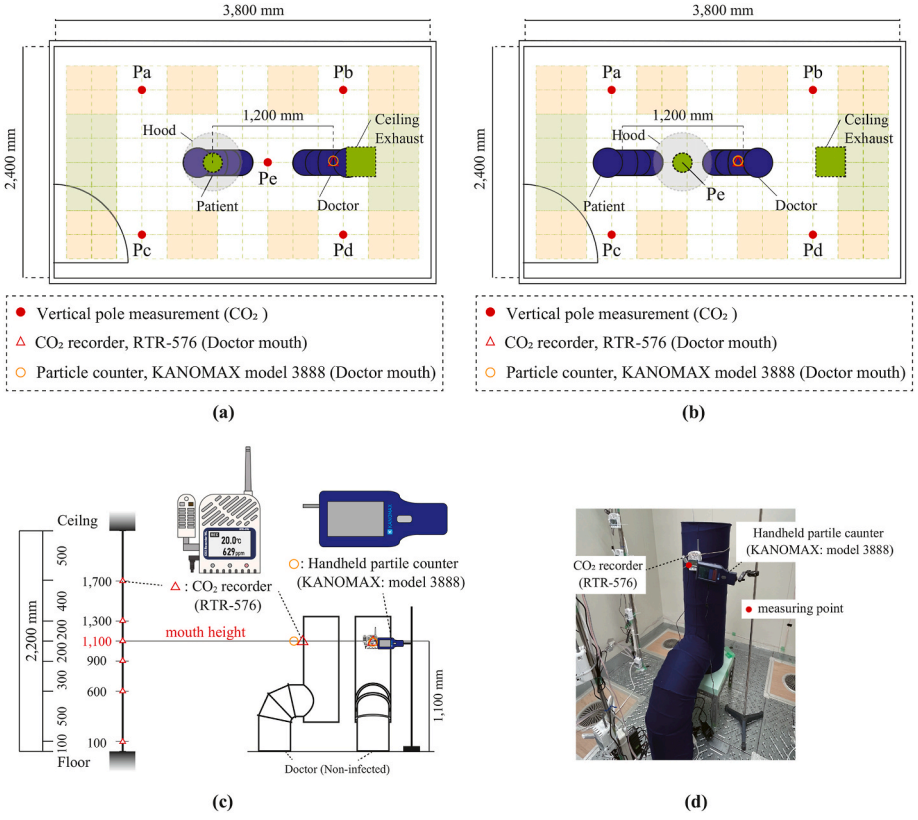

Fig. 6. Measurement points of CO_2 gas concentration (RTR-576, T&D Corporation) and particle (handheld particle counter: model 3888, KANOMAX). (a) Measurement plan view of Case A; hood_head. (b) Measurement plan view of Case B; hood_middle. (c) Vertical pole measurement points and doctor's mouth. (d) Pictures of measurements in front of the doctor's mouth.

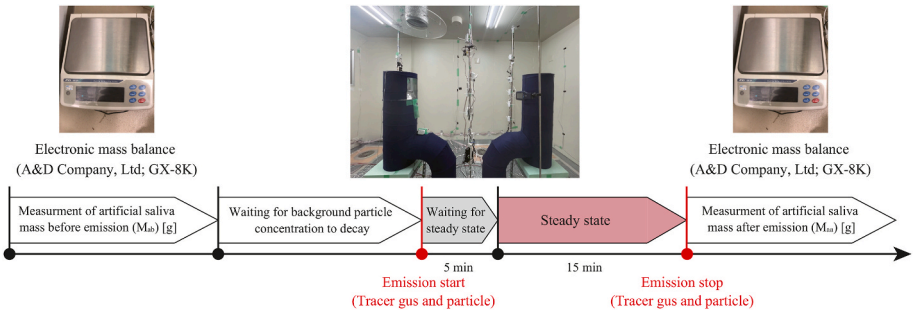

Fig. 7. Experiment procedures.

concentration was measured using a CO_2 recorder (RTR-576, T&D Corporation) in the exhaust duct.

2.4.2. Infection risk assessment

This study evaluated infection control performance using the Wells and Riley model [41,42]. The model defines one 'quanta' as the unit of infectivity that produces 63.2 % of new infections in a closed space, and the basic equation is expressed in Eq. (2).

$$P = 1 - e^{-n} \tag{2}$$

where P is the increased rate of the number of newly infected persons in a closed space, and n is the value of the quanta.

Based on the model, C_{qd}, the quanta concentration in front of the doctor's (non-infected person's) mouth [quanta/m^3] was calculated using Eqs. (3) and (5). Eq. (3) was used to calculate C_{qd} from the CO_2 gas.

$$C_{qd} = \frac{q}{Q} \bullet \frac{C_{dg}}{M_g/Q} \tag{3}$$

where q is the quanta emission rate (42 quanta/h), Q is the room ventilation rate [m^3/h], C_{dg} is the tracer gas concentration in front of the doctor's mouth [−], and M_g is the tracer gas (CO_2) emission rate (3.25 L/min). The average steady-state value over 15 min for each condition was used as the C_{dg} value. A quanta emission rate of 42 quanta/h calculated by REHVA [16] was used as the quanta production rate for infected persons during the conversation. Quanta emission rate values vary by disease and variant, with 42 quanta/h being the 90th percentile value for early variants of SARS-CoV-2 [16,43]. REHVA also shows that the quanta emission rate of omicron variants is approximately 2.5 times higher than that of the initial variants [44]; however, it was not necessary to use specific variants in this study because the purpose was to compare infection risk assessments using particles and gases. Additionally, because quanta emission rates contain a large degree of uncertainty, the infection risk presented in this study was only a reference value and can be considered statistically as the 90th percentile value for the initial variants of SARS-CoV-2. The CO_2 normalized concentration in front of the doctor's mouth, C_{nd} was calculated using Eq. (4). Because C_{nd} was normalized by the room concentration with perfect mixing, a C_{nd} of 1 indicated that the concentration at that point was equal to the concentration when the room air was perfectly mixed.

$$C_{nd} = \frac{C_{dg}}{M_g/Q} \tag{4}$$

The following two assumptions were made when calculating the risk of infection from the particles.

- Although the virus density per particle changed after evaporation, the total number of viruses does not change.
- The density of the virus during any evaporation process is constant regardless of particle size.

Eq. (5) was used to calculate C_{qd}, the quanta concentration in front of the doctor's (non-infected person's) mouth from the particles.

$$C_{qd} = \frac{q}{Q_{pt}} \bullet \frac{V_{dp}}{V_{ep}} \tag{5}$$

where C_{qd} represents the quanta concentration in front of the doctor's (non-infected person's) mouth [quanta/m^3], Q_{pt} is the volume flow rate of particle counter (2.81 L/min) [m^3/h], V_{dp} is the total volume of particles in front of the doctor's mouth measured by the particle counter (handheld particle counter: model 3888, KANOMAX) divided by measurement time (15 min) [m^3/h], and V_{ep} is the total generated volume of particles divided by emission time (20 min) [m^3/h]. As shown in Fig. 6, the emission and measurement times were different at 5 min because of the waiting time for a steady state. V_{ep} is defined by Eqs. (6) and (7).

$$V_{ep} = \frac{(M_{ab} - M_{aa}) \bullet R_c}{\rho_{aa}} \tag{6}$$

$$\rho_{aa} = \rho_{ab} \bullet R_c / R_d^3 \tag{7}$$

where M_{ab} is the mass of artificial saliva before emission [g], M_{aa} is the mass of artificial saliva after emission [g], R_c is compositional ratios of artificial saliva after evaporation to before evaporation [−], ρ_{aa} is the density of artificial saliva after evaporation [g/m^3], ρ_{ab} is the density of artificial saliva before evaporation (1.09 g/m^3), and R_d is the diameter ratio of particles after evaporation to before evaporation [−]. M_{ab} and M_{aa} were measured before and after the experiment using an electronic mass balance (GX-8K, A&D Company, Ltd), as shown in Fig. 7. Eq. (6) can be rewritten as Eq. (8), using Eq. (7).

$$V_{ep} = \frac{(M_{ab} - M_{aa}) \bullet R_d^3}{\rho_{ab}} \tag{8}$$

C_{qd}, the quanta concentration in front of the doctor's mouth [quanta/m^3] from the particles, was calculated using Eqs. (5) and (8). However, it must be assumed how much the particle size decreased due to evaporation (R_d). R_d was estimated by comparing the C_{qd} results calculated from the gas and particles in Section 3.2.

Using the value of C_{qd}, $t_{5\%}$, the time until the doctor's (non-infected person) infection risk reached 5 % was calculated from Eq. (9). Because the REHVA used a value of 5 % when describing a sufficiently low risk of infection in an office [16], this report also used 5 % as a reference for sufficiently low infection risk. As already discussed, this infection risk is an estimate for the initial variants of SARS-CoV-2, because 42 quanta/h was used as the quanta emission rate during conversations. The results of $t_{5\%}$ are discussed in Chapter 4.1.

$$t_{P\%} = -\frac{\ln(1-P)}{n \cdot P} \tag{9}$$

3. Results

3.1. Results calculated from CO_2 gas concentration

Fig. 8 shows the vertical distribution of CO_2 tracer gas concentration normalized by the flow-weighted concentrations of the two exhaust ducts for all 48 cases. Figs. 8 (a-1)–(a-3) compares the average values of Pa–Pd in Case A, where the hood was placed above the head of the infected person, for each hood exhaust flow rate. Pe was evaluated separately from Pa–Pd in Figs. 8 (c-1)–(d-3) because Pe was positioned in the middle of the mannequins. In the FSDV, a hood flow rate of 0 m3/h (black line) indicates that the normalized concentration was already low, and exhalation could be efficiently exhausted without a hood (Figs. 8 (a-1)). These results were due to the high ventilation rate of 1000 m^3/h (50 ACH). In the HFD, a displacement ventilation airflow field was observed, with the normalized concentration decreasing as the hood exhaust flow rate increased (Figs. 8 (a-2)). In the SFD, where the air was well mixed, the normalized concentration was close to 1, and it was observed that the normalized concentration decreased as the hood exhaust flow rate increased (Figs. 8 (a-3)). Fig. 8 (b-1)–(b-3) shows the average values of Pa–Pd of CO_2 normalized concentration for Case B, where the hood was placed in the middle of the mannequins. Comparing

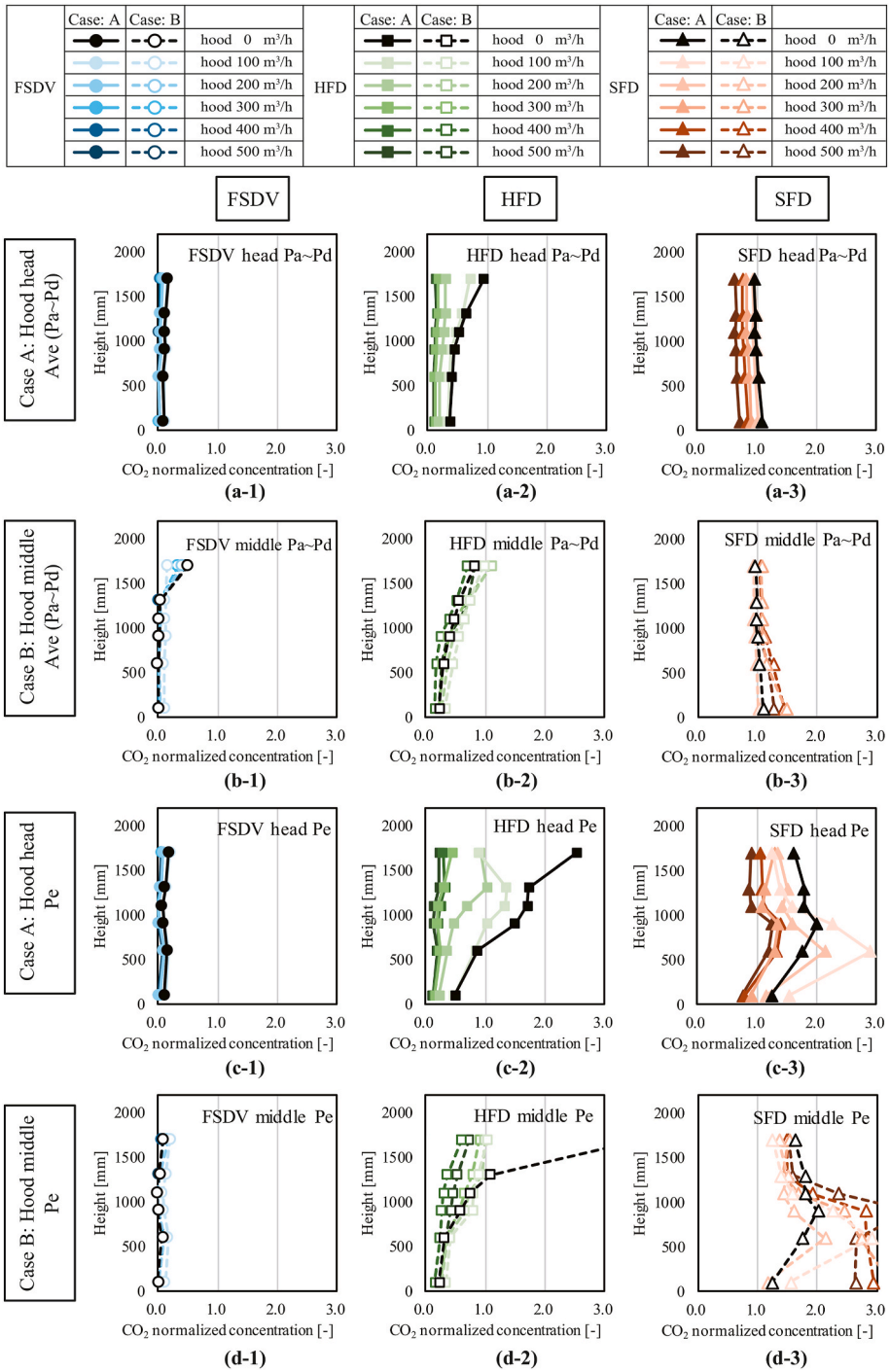

Fig. 8. Vertical distribution of normalized CO_2 concentration. Normalized by flow-weighted exhaust concentration. (a-1)–(b-3): Average results of Pa–Pd, showing the distribution of exhaled air in the room. (c-1)–(d-3): Results of Pe, showing the distribution of exhaled air between mannequins.

Figs. 8 (a-1)–(a-3), the normalized concentrations did not decrease significantly when the hood exhaust flow rate was increased.

Figs. 8 (c-1)–(d-3) shows the CO_2 normalized concentrations of Pe placed between the mannequins. The results for Pe under HFD (Figs. 8 (c-2) and (d-2)) and SFD (Figs. 8 (c-3) and (d-3)) conditions differed significantly from those for Pa–Pd (Figs. 8 (a-2), (b-2) and (a-3), (b-3)). In the HFD (Figs. 8 (c-2) and (d-2)), the CO_2 diffusion between the mannequins was reduced as the hood exhaust flow rate was increased. On the other hand, under SFD (Figs. 8 (c-2) and (d-2)) conditions, the concentration was higher around a height of 500 mm.

Fig. 9 (a) shows the hood capture efficiencies of the tracer gas in Cases A and B, calculated from the CO_2 tracer gas using Eq. (1). In the FSDV, the difference in η between Cases A and B is large. However, C_{qd}, the quanta concentration in front of the doctor's mouth shown in Fig. 9 (b) was low enough even in Case B, where η was low. In HFD, η in Case A was close to that of FSDV (Fig. 9 (a)). In Case A of the HFD, C_{qd} decreased as the hood exhaust flow rate increased; however, in Case B of the HFD, C_{qd} did not decrease to the same extent (Fig. 9 (b)). In SFD, η did not differ significantly between Cases A and B, suggesting that few exhalations were directly exhausted by the hood, and once spread throughout the room, they were exhausted by the hood and the ceiling exhaust (Fig. 9(a)). For C_{qd} of the SFD, the trend was similar to that of the HFD, with Case A confirming the effect of hood implementation and Case B showing that the effect of ambient airflow was more significant (Fig. 9 (b)).

3.2. Results calculated from artificial saliva particles

As mentioned in Section 2.4.2, Eqs. (5) and (8) were used to calculate the quanta concentration (C_{qd}) from the particles in front of the doctor's mouth. The amount of generated artificial saliva particles was estimated by measuring the decrease in artificial saliva before and after generation using an electronic mass balance (GX-8K, A&D Company, Ltd.), as shown in Fig. 7. When calculating the density, $R_{d,}$ the diameter ratio of the particles after evaporation to that before evaporation should be properly assumed. Previous studies by Yang et al. [45] have shown that the final particle size is 0.391–0.502 times smaller at a relative humidity of 10 %–90 %, as calculated by the experimental data of Tang et al. [46] and Bagger et al. [47]. These previous experiments were based on respiratory droplet size distributions; although the composition was different from that of the artificial saliva used in this experiment. Hence, C_{qd} was calculated by changing the values of R_d: 1.0, 0.40, 0.45, and 0.50, as shown in Fig. 10.

Fig. 10 (a) shows the comparison results of gas and particles by changing the assumed values of R_d for SFD. As the assumed R_d becomes smaller, V_{ep} in Eq. (5) decreases, resulting in a higher C_{qd}. When R_d was 1, the results calculated from the particles were significantly smaller than those calculated from CO_2; however, when R_d was 0.5, the two were in good agreement (Fig. 10(a)). When R_d was 0.45 and 0.4, the results calculated for the particles were larger than those calculated for CO_2. Considering the effects of adhesion and falling, the particle amount that reaches the doctor's mouth relative to the amount generated is expected to be smaller than that of gases. Therefore, in this study, R_d was assumed to be 0.5. In the HFD (Fig. 10 (b)), the calculated results of C_{qd} matched well for hood flow rates above 200 m^3/h when R_d was 0.5. However, for 50–150 m^3/h, C_{qd} calculated from the particles was lower than C_{qd} calculated from the gas. In the FSDV (Fig. 10 (c)), when R_d is 0.5, C_{qd} calculated from the gas is already small; thus, the comparisons on a linear scale seem to match (Figs. 10 (c-1)). However, when compared on a log scale vertical axis, the difference was 1.0×10^{-2} – 1.0×10^{-9} (Figs. 10 (c-2)).

Fig. 11 shows the results of C_{qd} calculated from the quanta concentration in front of the doctor's mouth calculated using artificial saliva particles ($R_d = 0.5$). Although the order of C_{qd} was matched or smaller than that calculated from CO_2, the trend was consistent; the risk of infection was lower in the order of FSDV < HFD < SFD. This was consistent with the order in which the indoor airflow became more turbulent. In Case A, the hood reduced the concentration in front of the doctor's mouth when the hood flow rate increased, as shown in Figs. 11 (a-2). However, when the hood was between the mannequins (Case B), the effect of the hood introduction was small because the hood exhaust flow rate and C_{qd} were not linearly related, as shown in Figs. 11 (a-2).

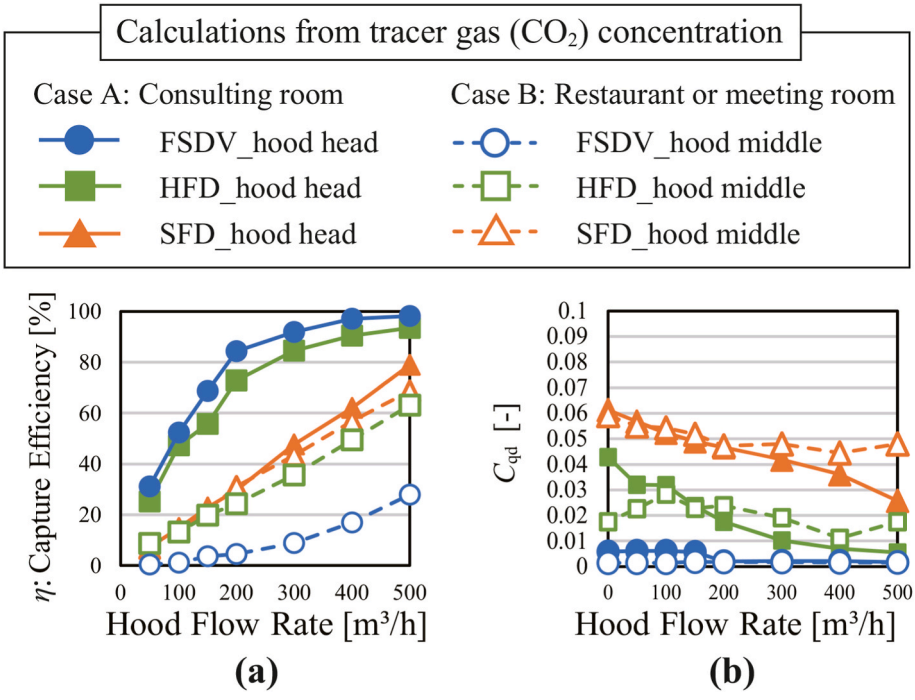

Fig. 9. Calculation results of (a) η: the hood CO_2 capture efficiency, (b) C_{qd}: quanta concentration in front of doctor's mouth calculated by tracer gas.

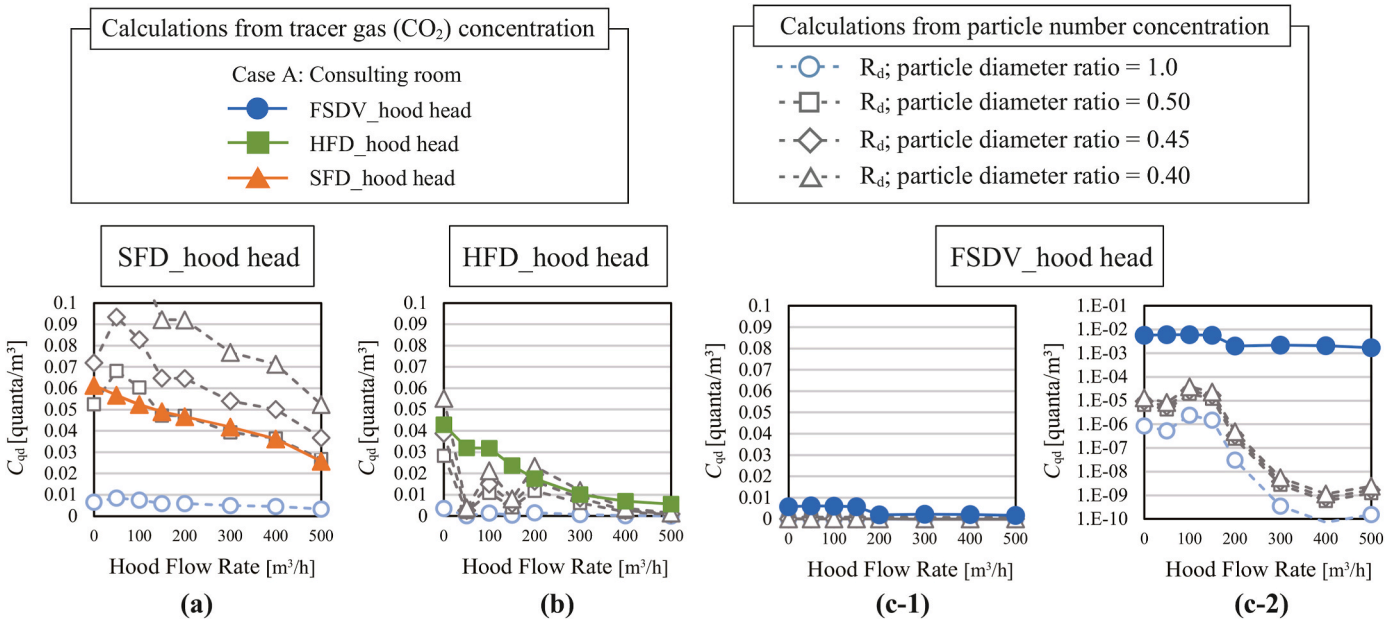

Fig. 10. Comparison of C_{qd} (quanta concentration in front of doctor's mouth) calculated by tracer gas concentration and particle number concentration of artificial saliva changing R_d; the diameter ratio of particles after evaporation to before evaporation [−] from 1.0 to 0.4. (a) SFV_hood head. (b) HFD_hood head. (c-1) FSDV_hood head, linear vertical axis. (c-2) FSDV_hood head, log scaling vertical axis.

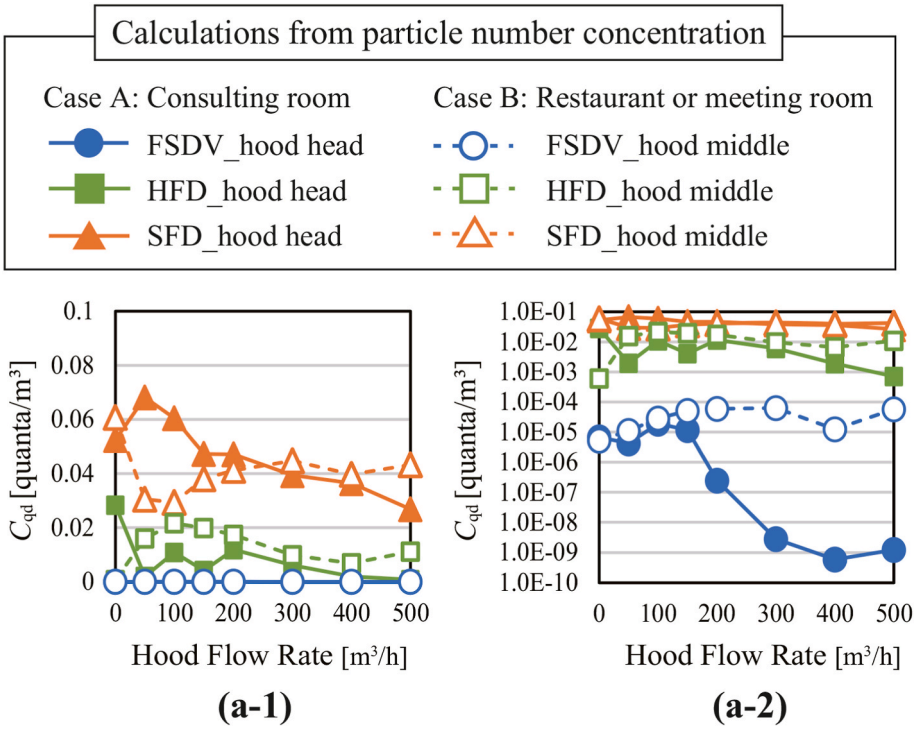

Fig. 11. Calculation results of (a) C_{qd}: quanta concentration in front of doctor's mouth (R_d = 0.5). (a-1) C_{qd} in a linear vertical axis. (a-2) C_{qd} in a log scaling vertical axis.

4. Discussion

4.1. Summarize the essential findings

Section 3 presents the indoor distribution of the CO2 gas normalized concentration in Fig. 8, η the tracer gas capture efficiency, and C_{qd} the quanta concentrations in front of the non-infected person's mouth calculated from CO_2 gas in Fig. 9. The C_{qd} calculated from the particles is also presented in Figs. 10 and 11. Findings from the CO_2 gas results presented in Figs. 8 and 9 are summarized below.

- The FSDV could exhaust the exhaled air of infected persons without spreading it, regardless of the hood flow rate.
- In the HFD, although there was more exhalation diffusion than in the FSDV due to horizontal airflow, increasing the hood flow rate

allowed the CO_2 normalized concentration to close to zero for the entire room.
- In the SFD, the exhaled air diffuses widely in the room due to the swirling airflow, and increasing the hood flow rate does not significantly affect the concentration in front of the doctor's mouth.
- In the HFD and the SFD, the CO_2 concentration distributions between the middle of humans and in the room differed significantly. In SFD, it was also suggested that there was a downward airflow middle of humans.

In Figs. 10 and 11, the results of C_{qd} the quanta concentrations in front of the non-infector's mouth calculated from the particles are shown. Compared to the gas results in Fig. 10, the final diameter of the artificial saliva particles was assumed to be half that before evaporation ($R_d = 0.5$). Findings from the artificial saliva particles are summarized below.

- The quieter the indoor airflow, the greater the effect of deposition, resulting in the C_{qd} of particles becoming smaller than that of CO_2 gases.
- Because CO_2 assessed the infection risk higher than particles, it is on the safe side as an airborne infection risk assessment method.

Common features of the gas and particle results also indicated the following.

- As the performance of hoods was greatly influenced by the ambient airflow, ventilation systems that can form a calm upward airflow, such as SFDV, are ideal for use with hoods.
- When the hood was above the infector's head, the hood airflow contributed to reducing the C_{qd}, whereas when it was middle of humans, it had little effect on the C_{qd}.

The relationship between LEV, exhaled diffusion and quanta concentration of non-infected persons is discussed above. In the following, the infection risk for the initial variants of SARS-CoV-2 is estimated using Eq. (9), and the safety of the present system against airborne infections is discussed.

Fig. 12 shows the results of $t_{5\%}$, the time until the doctor's infection probability reaches 5 %, calculated from the CO_2 tracer gas using Eq. (9). This infection risk is an estimate for the initial variants of SARS-CoV-2 because 42 quanta/h was used as the quanta emission rate during the conversation, as discussed in Section 2.4.2. In the FSDV, the value of $t_{5\%}$ consistently exceeded 24 h, which is sufficiently safe against airborne infection. In the HFD, when the hood flow rate was over 200 m^3/h, the $t_{5\%}$ value exceeded 8 h and can be considered relatively safe, which is assumed to be the maximum value of working hours. In contrast, in the SFD, the value of $t_{5\%}$ does not always exceed 8 h and cannot be regarded as sufficiently safe.

Fig. 13 shows $t_{5\%}$, the time until the doctor's infection probability reached 5 %, calculated using artificial saliva particles ($R_d = 0.5$). The $t_{5\%}$ shown in Fig. 13 was similar to that calculated for the gas in Fig. 12, and the risk of airborne infection was sufficiently low even without a hood in the FSDV. In HFD, introducing hoods could extend $t_{5\%}$ for 8 h or more, whereas in SHD, even with hoods, $t_{5\%}$ was less than 8 h, and there was a non-negligible risk of infection.

4.2. Compare the findings to the previous study

This experiment was carried out at 50 ACH due to the limitations of the experimental setup. In the experiment by J. Yang et al. on personal exhaust systems [23], the performance of personalized exhaust did not differ much between MV and DV under typical airflow rates, suggesting that ambient airflow may have had an excessive influence on the results of this paper. The authors' CFD analysis [34] also showed that the introduction of LEV at 6–12 ACH in FSDV significantly reduced the risk of infection in doctors compared to without LEV. This suggests that LEV may work effectively in experiments at 4–12 ACH, even in MV and DV. A practical implication of this experiment is that even under high ventilation volumes (50 ACH), the FSDV can create a calm upward airflow, which reduces the horizontal distribution of the patient's exhaled air and prevents airborne infection. These results can be applied to super-clean rooms in hospitals, factories for semiconductors, etc., and

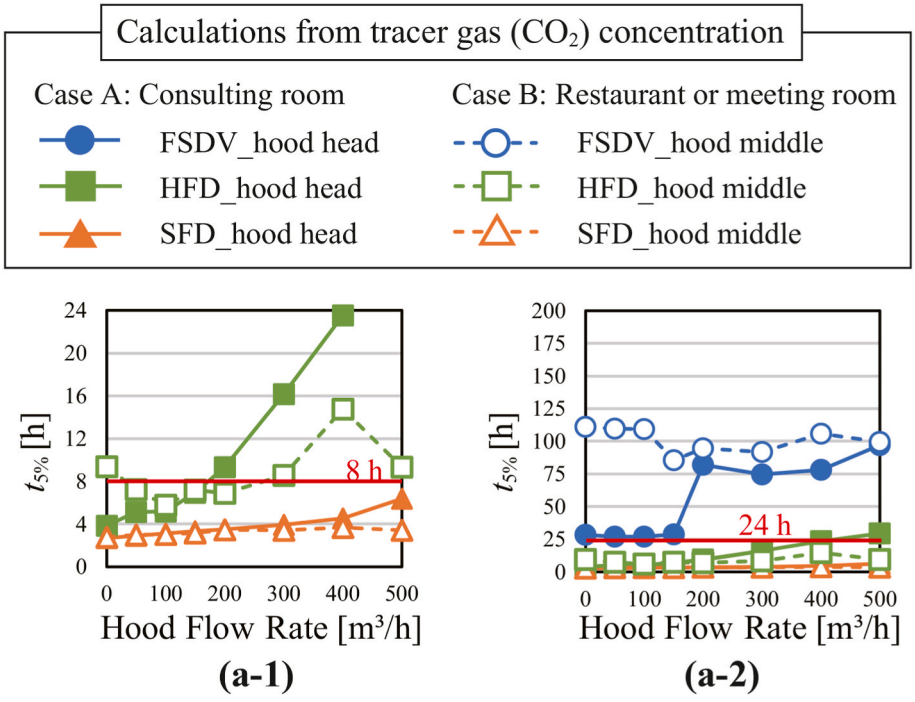

Fig. 12. Calculation results of $t_{5\%}$: time until doctor's infection probability reaches 5 % calculated by tracer gas. (a-1) The maximum value of the vertical axis is 24 h. (a-2) The maximum value of the vertical axis is 200 h.

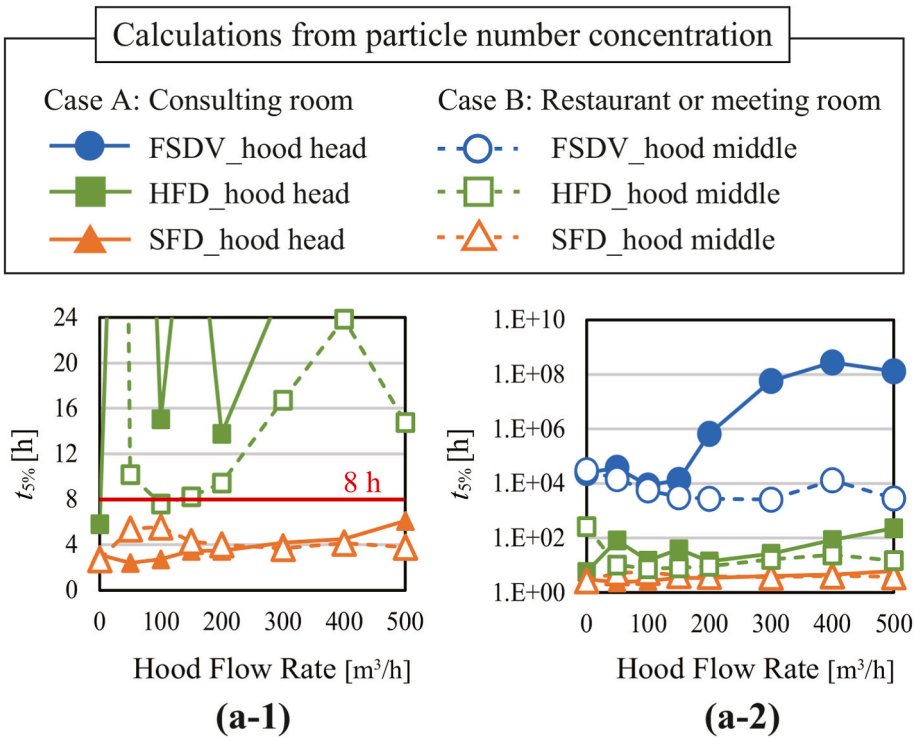

Fig. 13. Calculation results of $t_{5\%}$: time until doctor's infection probability reaches 5 %, calculated by artificial saliva particle ($R_d = 0.5$). (a-1) $t_{5\%}$ in a linear vertical axis. (a-2) $t_{5\%}$ in a log scaling vertical axis.

biological research facilities, etc., where large ventilation volumes are required. Also, in the HFD, when ventilation volumes are high (50 ACH), the risk of airborne transmission of infection through conversation can be sufficiently low by introducing a hood. However, in the SFD, the introduction of hoods does not sufficiently reduce the risk of airborne transmission of infection under 50ACH. This would apply not only to the SFD but also to other factors causing significant turbulence in the vicinity of the patient, e.g. a fan. In addition, the present results should be adapted to smaller spaces such as examination rooms and meeting rooms, since in large spaces the distance between floor diffusers might be larger and the mutual influence of the airflows might be smaller.

In this study, only the exhalation of patients was considered in steady-state conditions, whereas in the study by J. Yang et al. [23] non-steady state experiments were carried out considering the inhalation of non-infected persons. In our research, the average initial velocity of exhalation during the speech, i.e. 0.30 m/s, obtained in previous studies [34], was used to simulate the time-averaged conversation. The inhalation might increase the infection risk assessment, however, according to CFD and an experimental review of micro-climate around the human body by S. Murakami [48], 90 % of the air near the mouth is inhaled, while less than 10 % is inhaled near the chest. The influence of ambient airflow on the infection risk assessment is greater than that of the inhalation because of the higher ventilation volume, i.e. 50 ACH. In addition, as there is an inhalation, exhalation, and pause process in the non-steady state, the risk of infection is not necessarily greater than in our conditions, which are an average of these conditions. However, as few experiments are comparing them, future comparisons of infection risk assessment should be made under low ventilation rates, considering nasal or oral inhalation. For the infection risk assessment, the $t_{5\%}$ was calculated with time as a variable, because the exposure duration is varied for different situations. The $t_{5\%}$ was more than 8 h for HFD and FSDV and less than 8 h for SFD. These results might be influenced by the initial velocity of the exhaled air of an infected person or the inhaled air of a non-infected person, but this does not affect the conclusions as the study focuses on relative comparisons of methods.

4.3. Limitations

This study had several limitations.

- As mentioned in Section 1, the ventilation rate was 1000 m^3/h (50 ACH). Therefore, the air supply method had a greater impact on the results than the hood. Future experiments using general ventilation levels are required. In this case, even if the hood was placed slightly farther away from the source, there could be a certain hood-introduction effect.
- R_d; the diameter ratio of particles after evaporation to before evaporation [−] was assumed by comparing the results with those calculated from CO_2 in Fig. 12, although R_d should be determined based on indoor humidity and other factors. However, no data are available on the R_d of the artificial saliva used in this study, and it is difficult to measure the particle size after evaporation when the particles are released into the air.
- The behavior of particles and gases can only be estimated from the concentration before the doctor's mouth and requires further investigation through visualization experiments using Particle Image Velocimetry or unsteady analysis using Computational Fluid Dynamics.
- As the experiment was conducted for 15 min after a steady state, long-term cumulative effects such as particle accumulation in different parts of the room could not be taken into account. In practice, there are factors such as filter clogging and mechanical wear that can reduce the exhaust flow rate of LEVs. As the results show that food flow rates have a significant impact on infection control performance, attention should be paid to the long-term effects.
- Although the Particle size distribution of artificial saliva is not significantly different compared to Morawsaka's results [40] (see Appendix A), it differs in composition from real saliva. In particular, the use of glycerol to reproduce viscosity may have overestimated the adhesive strength of walls and ceilings.

4.4. Present a way forward

In the experiments with general ventilation rates (4–12 ACH), LEV may work effectively even when the background ventilation is MV, and future experiments are required with the volume and type of ambient airflow as a parameter.

A simple Wells-Riley model was used as a measure of infection risk assessment, but the effects of viral inactivation and deposition can also be considered. REHVA [16] estimates that the impact of deposition is 0.3 1/h [49,50] and the impact of viral inactivation is 0.32 1/h [51], which is sufficiently small compared to the ventilation rate of this study, i.e. 50 1/h. Not taking them into account leads to a larger assessment of transmission risk, therefore the results of this study assess the safety side. However, in the future, more accurate assessments are expected to be made using the extended Wells-Riley model, which considers deposition and viral inactivation as in A. Aganovic et al. [52] and W. Liu et al. [53] under generally smaller ventilation volumes. In addition, non-steady state experiments that simulate the exhalation and inhalation of humans can reproduce more realistic conditions.

5. Conclusion

This study evaluated the performance of local exhaust ventilation systems (hoods) used in factories and kitchens as airborne infection control measures. The parameters were the hood exhaust flow rate and three types of underfloor air distribution systems. Air supply methods such as floor-supply displacement ventilation (FSDV), horizontal flow floor diffusers (HFD), and swirling flow floor diffusers (SFD) were compared. In Case A, the hood was placed above the patient's (infected person's) head in the consultation (examination) room, and in Case B, the hood and desk were placed in the middle of the mannequins in the restaurant or meeting room. The differences in infection risk assessment between the use of CO_2 and artificial saliva particles as tracers of exhaled breath were discussed. The findings of this study are summarized as follows.

- The distribution of vertical normalized concentrations and the results of quanta concentrations in front of the doctor's mouth indicate that the distribution of exhaled air into the room and the infection risk for the doctor decreased in the order FSDV < HFD < SFD. This is consistent with the order in which indoor airflow becomes more turbulent. Since the air supply area of FSDV is larger than with diffusers, the average indoor airflow can be reduced. Therefore, FSDVs are preferable to HFDs and SFDs for airborne infection control.
- In Case A, which involved consulting rooms, the effect of introducing hoods was confirmed to a certain degree across all three ventilation methods. However, in Case B, encompassing restaurants or meeting rooms, the effect of hoods on the infection risk of individuals facing them was small. In particular, in Case A_FSDV, the effect of installing a hood was significant, and the use of the FSDV and LEV in the consulting room was reasonable.
- Comparing the airborne infection risk assessment between gas and particles, gas appears to offer greater safety in terms of airborne infection prevention because it evaluates higher quanta concentration in front of the doctor's mouth [quanta/m^3]. In the SFDV, the risk assessment of airborne infection by particles was smaller than that of gas because of the greater impact of particle adhesion and falling.

A practical implication of this experiment is that even under high ventilation volumes (50 ACH), the FSDV can create a calm upward airflow, which reduces the horizontal distribution of the patient's exhaled air and prevents airborne infection. These results can be applied to super-clean rooms in hospitals, factories for semiconductors, etc., and biological research facilities, etc., where large ventilation volumes are required. In addition, the results of this study should be adapted to smaller spaces such as examination rooms and meeting rooms, since in large spaces the distance between floor diffusers might be larger and the mutual influence of the airflows might be smaller.

Data sharing and data accessibility

Data supporting the findings of this study are available from the corresponding author upon request.

CRediT authorship contribution statement

Jun Yoshihara: Writing – original draft, Visualization, Methodology, Investigation, Data curation. **Toshio Yamanaka:** Writing – review & editing, Supervision, Project administration, Funding acquisition, Conceptualization. **Narae Choi:** Supervision. **Tomohiro Kobayashi:** Supervision. **Noriaki Kobayashi:** Software, Resources. **Aoi Fujiwara:** Visualization, Methodology, Investigation, Data curation.

Declaration of competing interest

The authors declare that they have no competing financial interests or personal relationships that may have influenced the work reported in this study.

Data availability

Data will be made available on request.

Acknowledgements

This study was supported by a JSPS Grant-in-Aid for Scientific Research in Japan (B)21H0149 and an Osaka University School of Medicine Research and Development Grant for Novel Coronavirus Countermeasures in 2021. In Appendix A, the particle size distribution of the ultrasonic nebulizers was measured using PALAS: Welas Digital 2000, with the cooperation of the Tokyo Dylec Corporation, Ltd. We hereby express our appreciation. Also, the authors would like to thank Editage (www.editage.com) for English language editing.

Appendix A. Nebulizer performance measurement

The ultrasonic nebulizer (SHIN-EI INDUSTRIES, Inc. Comfort 3000, KU-500) was developed for medical rather than experimental purposes. Therefore, we measured the particle size distribution to confirm the reproducibility of human-derived droplets while speaking. Fig. A1 shows the measurement system, PALAS: Welas Digital 2000, which uses the principle of light scattering. The instrument can measure up to a high concentration ($<10^6$ 1/cm^3) without a diluter. This allowed us to obtain the results with minimal evaporation effect. The nebulizer was supplied with air at a rate of 5.21 L/min, consistent with the experimental conditions. The measurement was performed three times for 60 s, and the particle size distribution and number concentration were recorded. Particle size distribution was calculated using Eqs. (A.1) and (A.2) for comparison with a previous study by Morawska et al. [40]. The measurement range was 0.2–10 μm, divided into 32 intervals.

$$dC_{ni} / d\,log_{10}D_i = n_i / V_m / \Delta log_{10}D_i \quad \text{(A.1)}$$

$$\Delta log_{10}D_i = log_{10}D_{i,upper} - log_{10}D_{i,lower} \quad (A.2)$$

where C_{ni} is the particle number concentration for each interval [m^{-3}]; D_i is the arithmetic interval width [m], n_i is the measured number of particles within the interval borders $D_{i,\ upper}$ and $D_{i,\ lower}$ [p], V_m is the measured volume [m^3], $D_{i,\ upper}$ is the diameter of the upper interval border [m], and $D_{i,\ upper}$ is the diameter of the lower interval border [m].

Eq. (A.3) calculated the number concentration, and the total value was calculated by summing each interval width.

$$Sum\ dC_{ni} = \sum n_i \Big/ V_m \quad (A.3)$$

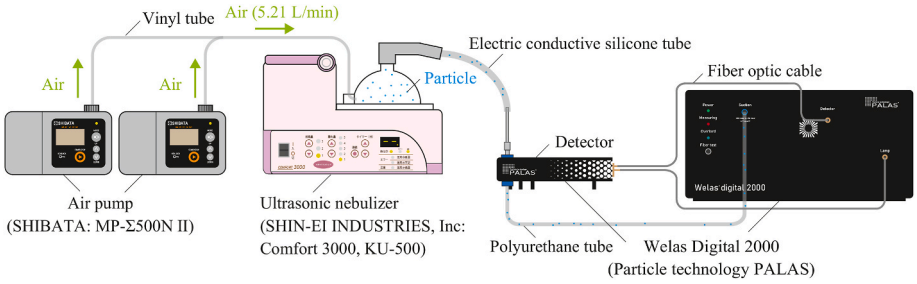

Fig. A.1. Measurement system for particle size distribution and number concentration of ultrasonic nebulizer.

The measurement results are presented in Fig. A2. Background noise ranged from 10 to 100 cm^{-3} below 1 μm, which was negligibly small compared to the nebulizer measurement of a5 × 10^5. Fig. A2 (a) shows the average of three measurements of the particle size distribution. There is one peak at 0.2–0.3 μm and another at 1–1.1 μm. Morawska et al. measured particles of human origin during voiced counting using the Expiratory Droplet Investigation System (EDIS) and found a single peak at 0.8 μm [40]; however, they measured particles after water had evaporated a short time after emission from a mouth, and considering this effect, the 1–1.1 μm peak of the ultrasonic nebulizer could be close to that of droplets from voiced counting. For the smaller peak (0.2–0.3 μm), because the particle counter (KANOMAX: model 3888) used to measure the particles in front of the doctor's mouth in the main experiment had a measurement range of 0.3 μm or larger, it is highly possible that those particles from this peak were not measured in the main experiment, considering the effect of evaporation. However, since the volume of particles of 0.2–0.3 μm is $1/5^3$ compared to particles of 1–1.1 μm, the impact of the missing measurement of particles of 0.2–0.3 μm on the infection risk assessment is considered to be small. In Fig. A2(b), the number concentration was 4–5 × 10^5, indicating that sufficient quantities of tracer particles were generated.

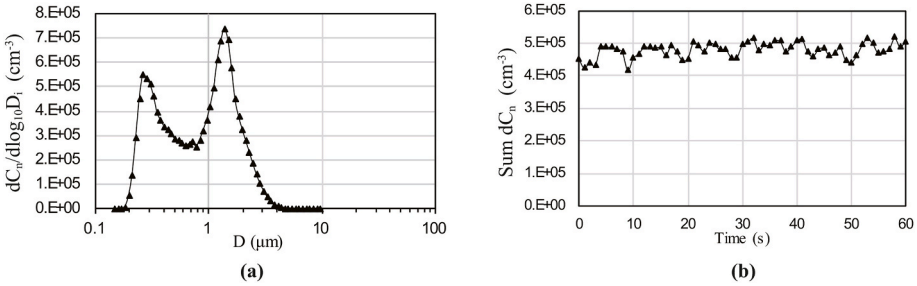

Fig. A.2. Measurement results of (a) particle size distribution averaged three times (60 s each time) and (b) particle number concentration of the ultrasonic nebulizer (extracted one time randomly).

References

[1] World Health Organization, WHO COVID-19 dashboard, n.d. https://data.who.int/dashboards/covid19/cases?n=c. (Accessed 2 April 2024).

[2] World Health Organization, COVID-19 epidemiological update, Edition 165 published 15 March 2024, https://www.who.int/publications/m/item/covid-19-epidemiological-update-15-march-2024, 2024. (Accessed 2 April 2024).

[3] M.L. Ranney, V. Griffeth, A.K. Jha, Critical supply shortages — the need for ventilators and personal protective equipment during the Covid-19 pandemic, N. Engl. J. Med. 382 (2020) e41, https://doi.org/10.1056/nejmp2006141.

[4] T.M. Cook, Personal protective equipment during the coronavirus disease (COVID) 2019 pandemic – a narrative review, Anaesthesia 75 (2020) 920–927, https://doi.org/10.1111/anae.15071.

[5] D. Lewis, Is the coronavirus airborne? Experts can't agree, Nature 580 (2020) 175, https://doi.org/10.1038/D41586-020-00974-W.

[6] T. Greenhalgh, J.L. Jimenez, K.A. Prather, Z. Tufekci, D. Fisman, R. Schooley, Ten scientific reasons in support of airborne transmission of SARS-CoV-2, Lancet 397 (2021) 1603–1605, https://doi.org/10.1016/S0140-6736(21)00869-2.

[7] C.J. Heneghan, E.A. Spencer, J. Brassey, A. Plüddemann, I.J. Onakpoya, J.L. Oke, D.H. Evans, J.M. Conly, T. Jefferson, N.H.L. Leung, H. Kong, M. Yao, SARS-CoV-2 and the role of airborne transmission: a systematic review [version 3; peer review: 1 approved with reservations, 2 not approved], https://doi.org/10.12688/f1000research.52091.1, 2021.

[8] L. Morawska, D.K. Milton, It is time to Address airborne transmission of coronavirus disease 2019 (COVID-19), Clin. Infect. Dis. 71 (2020) 2311–2313, https://doi.org/10.1093/CID/CIAA939.

[9] S. Tang, Y. Mao, R.M. Jones, Q. Tan, J.S. Ji, N. Li, J. Shen, Y. Lv, L. Pan, P. Ding, X. Wang, Y. Wang, C.R. MacIntyre, X. Shi, Aerosol transmission of SARS-CoV-2? Evidence, prevention and control, Environ. Int. 144 (2020), https://doi.org/10.1016/J.ENVINT.2020.106039.

[10] P. Azimi, Z. Keshavarz, J.G. Cedeno Laurent, B. Stephens, J.G. Allen, Mechanistic transmission modeling of COVID-19 on the Diamond Princess cruise ship demonstrates the importance of aerosol transmission, Proc. Natl. Acad. Sci. U.S.A. 118 (2021), https://doi.org/10.1073/PNAS.2015482118/-/DCSUPPLEMENTAL.

[11] Y. Li, H. Qian, J. Hang, X. Chen, P. Cheng, H. Ling, S. Wang, P. Liang, J. Li, S. Xiao, J. Wei, L. Liu, B.J. Cowling, M. Kang, Probable airborne transmission of SARS-CoV-2 in a poorly ventilated restaurant, Build. Environ. 196 (2021) 107788, https://doi.org/10.1016/J.BUILDENV.2021.107788.

[12] World Health Organization, Coronavirus disease (COVID-19): how is it transmitted?. https://www.who.int/emergencies/diseases/novel-coronavirus-2019/question-and-answers-hub/q-a-detail/coronavirus-disease-covid-19-how-is-it-transmitted, 2021. (Accessed 17 November 2022).

[13] J.L. Domingo, M. Marquès, J. Rovira, Influence of airborne transmission of SARS-CoV-2 on COVID-19 pandemic, A Rev. Environ. Res. 188 (2020), https://doi.org/10.1016/j.envres.2020.109861.
[14] C.C. Wang, K.A. Prather, J. Sznitman, J.L. Jimenez, S.S. Lakdawala, Z. Tufekci, L. C. Marr, Airborne transmission of respiratory viruses, Science (1979) 373, https://doi.org/10.1126/science.abd9149, 2021.
[15] World Health Organization, Natural Ventilation for Infection Control in Health-Care Settings, World Health Organization, 2009. https://www.who.int/publications/i/item/9789241547857. (Accessed 1 May 2024).
[16] Federation of European Heating Ventilation and Air Conditioning Associations, COVID-19 Guidance Document Version 4.0; How to Operate HVAC and Other Building Service Systems to Prevent the Spread of the Coronavirus (SARS-CoV-2) Disease (COVID-19) in Workplaces, 2020.
[17] Y. Liu, C. Li, H. Ma, X. Luo, Performance of local supply-exhaust ventilation around stove with numerical simulation in a residential kitchen, J. Build. Eng. 87 (2024), https://doi.org/10.1016/j.jobe.2024.109078.
[18] B. Elihollund, B.E. Moen, Chemical exposure in hairdresser salons; effect of local exhaust ventilation, Ann. Occup. Hyg. 42 (1998) 277–281, https://doi.org/10.1093/annhyg/42.4.277.
[19] K. Logachev, A. Ziganshin, O. Kryukova, O. Averkova, I. Kryukov, A. Gol'tsov, Improving dust capture efficiency with local exhaust hoods in manicure shops, Build. Environ. 181 (2020), https://doi.org/10.1016/j.buildenv.2020.107124.
[20] ASHRAE, ASHRAE applications handbook (Chapter 29) - Industrial Local Exhaust Systems, https://www.ashrae.org/advertising/handbook-advertising/applications/industrial-local-exhaust, 1999. (Accessed 5 April 2024).
[21] M.R. Flynn, P. Susi, Local exhaust ventilation for the control of welding fumes in the construction industry - a literature review, Ann. Occup. Hyg. 56 (2012) 764–776, https://doi.org/10.1093/annhyg/mes018.
[22] A.K. Melikov, Personalized ventilation, Indoor Air 14 (2004) 157–167, https://doi.org/10.1111/J.1600-0668.2004.00284.X.
[23] J. Yang, S.C. Sekhar, K.W.D. Cheong, B. Raphael, Performance evaluation of a novel personalized ventilation-personalized exhaust system for airborne infection control, Indoor Air 25 (2015) 176–187, https://doi.org/10.1111/ina.12127.
[24] C. Xu, X. Wei, L. Liu, L. Su, W. Liu, Y. Wang, P.V. Nielsen, Effects of personalized ventilation interventions on airborne infection risk and transmission between occupants, Build. Environ. 180 (2020) 107008, https://doi.org/10.1016/J.BUILDENV.2020.107008.
[25] B. Rahmati, A. Heidarian, A.M. Jadidi, The relation between airflow pattern and indoor air quality in a Hybrid personalized ventilation with under-floor air distribution system, Exp. Tech. (2022) 1–20, https://doi.org/10.1007/S40799-022-00595-0/TABLES/6.
[26] A. Melikov, A. Li, R. Kosonen, X. Li, Occupant targeted ventilation brings clean air to occupants, The REHVA Eur. HVAC J. (2022). https://www.researchgate.net/publication/358915595.
[27] M. Komori, T. Yamanaka, T. Kobayashi, N. Choi, N. Kobayashi, Y. Suzuki, Study on capture performance of local exhaust hood under passing airflow, J. Environ. Eng. 88 (2023) 587–596, https://doi.org/10.3130/aije.88.587 (in Japanese).
[28] B.W. Olesen, M. Koganei, G.T. Holbrook, J.E. Woods, Evaluation of a vertical displacement ventilation system, Build. Environ. 29 (1994) 303–310.
[29] T. Akimoto, T. Nobe, S. Tanabe, K. Kimura, Experimental study on indoor thermal environment and ventilation performance of floor-supply displacement ventilation system, J. Architect. Plann. (Transact. AIJ) 62 (1997) 17–25, https://doi.org/10.3130/AIJA.62.17_3.
[30] J. Lau, Q. Chen, Floor-supply displacement ventilation for workshops, Build. Environ. 42 (2007) 1718–1730, https://doi.org/10.1016/j.buildenv.2006.01.016.
[31] X. Yuan, Q. Chen, L.R. Glicksman, A Critical Review of Displacement Ventilation, 1998, pp. 1–13. AIVC 4101, https://www.aivc.org/resource/critical-review-displacement-ventilation. (Accessed 26 November 2022).
[32] P. V Nielsen, Displacement Ventilation - Theory and Design, Aalborg University, 1993. https://vbn.aau.dk/ws/portalfiles/portal/36323578/Displacement+Ventilation+-+theory+and+design+%28gul+serie%29.pdf. (Accessed 24 May 2024).
[33] K. Zhang, X. Zhang, S. Li, X. Jin, Review of underfloor air distribution technology, Energy Build. 85 (2014) 180–186, https://doi.org/10.1016/J.ENBUILD.2014.09.011.
[34] J. Yoshihara, T. Yamanaka, T. Kobayashi, N. Choi, N. Kobayashi, Performance of combination of local exhaust system and floor-supply displacement ventilation system as prevention measure of infection in consulting room, Japan Architect. Rev. 6 (2023), https://doi.org/10.1002/2475-8876.12413.
[35] E. Bjørn, P.V. Nielsen, Dispersal of exhaled air and personal exposure in displacement ventilated rooms, Indoor Air 12 (2002) 147–164, https://doi.org/10.1034/j.1600-0668.2002.08126.x.
[36] Y. Bi, A. Aganovic, H.M. Mathisen, G. Cao, Experimental study on the exposure level of surgical staff to SARS-CoV-2 in operating rooms with mixing ventilation under negative pressure, Build. Environ. 217 (2022), https://doi.org/10.1016/j.buildenv.2022.109091.
[37] A. Essa, T. Yamanaka, T. Kobayashi, N. Choi, Effect of source location on contaminant dispersion pattern and occupants inhaled air quality in lecture room under displacement ventilation, Japan Architect. Rev. 6 (2023), https://doi.org/10.1002/2475-8876.12313.
[38] World Health Organization, Transmission of SARS-CoV-2: Implications for Infection Prevention Precautions, World Health Organization, 2020.
[39] M. Ogata, M. Ichikawa, H. Tsutsumi, T. Ariga, S. Hori, S.I. Tanabe, Measurement of cough droplet deposition using the cough machine, J. Environ. Eng. 83 (2018) 57–64, https://doi.org/10.3130/aije.83.57 (in Japanese).
[40] L. Morawska, G. Johnson, Z. Ristovski, M. Hargreaves, K. Mengersen, S. Corbett, C. Chao, Y. Li, D. Katoshevski, Size distribution and sites of origin of droplets expelled during expiratory activities. http://eprints.qut.edu.au/, 2009.
[41] W.F. Wells, M.W. Wells, T.S. Wilder, The environmental control of epidemic contagion 1. An epidemiologic study of radiant disinfection of air in day schools. https://academic.oup.com/aje/article/35/1/97/85502, 1942.
[42] E.C. Riley, G. Murphy, R.L. Riley, Airborne spread of measles in a suburban elementary school, Am. J. Epidemiol. 107 (1978) 421–432.
[43] G. Buonanno, L. Stabile, L. Morawska, Estimation of airborne viral emission: quanta emission rate of SARS-CoV-2 for infection risk assessment, Environ. Int. 141 (2020), https://doi.org/10.1016/j.envint.2020.105794.
[44] REHVA, REHVA COVID-19 ventilation calculator documentation Version 2.0 updates, n.d. https://www.rehva.eu/covid19-ventilation-calculator. (Accessed 29 March 2024).
[45] W. Yang, L.C. Marr, Dynamics of Airborne influenza A viruses indoors and dependence on humidity, PLoS One 6 (2011), https://doi.org/10.1371/journal.pone.0021481.
[46] I.N. Tang, A.C. Tridico, K.H. Fung, Thermodynamic and optical properties of sea salt aerosols, J. Geophys. Res. Atmos. 102 (1997) 23269–23275, https://doi.org/10.1029/97jd01806.
[47] H.L. Bagger, C.C. Fuglsang, P. Westh, Hydration of a glycoprotein: relative water affinity of peptide and glycan moieties, Eur. Biophys. J. 35 (2006) 367–371, https://doi.org/10.1007/s00249-005-0035-5.
[48] S. Murakami, Analysis and design of micro-climate around the human body with respiration by CFD, Indoor Air 14 (2004) 144–156, https://doi.org/10.1111/J.1600-0668.2004.00283.X.
[49] T.L. Thatcher, A.C.K. Lai, R. Moreno-Jackson, R.G. Sextro, W.W. Nazaroff, Effects of Room Furnishings and Air Speed on Particle Deposition Rates Indoors, 2002.
[50] E. Diapouli, A. Chaloulakou, P. Koutrakis, Estimating the concentration of indoor particles of outdoor origin: a review, J. Air Waste Manage. Assoc. 63 (2013) 1113–1129, https://doi.org/10.1080/10962247.2013.791649.
[51] N. van Doremalen, T. Bushmaker, D.H. Morris, M.G. Holbrook, A. Gamble, B. N. Williamson, A. Tamin, J.L. Harcourt, N.J. Thornburg, S.I. Gerber, J.O. Lloyd-Smith, E. de Wit, V.J. Munster, Aerosol and surface stability of SARS-CoV-2 as compared with SARS-CoV-1, N. Engl. J. Med. 382 (2020) 1564–1567, https://doi.org/10.1056/nejmc2004973.
[52] A. Aganovic, Y. Bi, G. Cao, F. Drangsholt, J. Kurnitski, P. Wargocki, Estimating the impact of indoor relative humidity on SARS-CoV-2 airborne transmission risk using a new modification of the Wells-Riley model, Build. Environ. 205 (2021), https://doi.org/10.1016/j.buildenv.2021.108278.
[53] W. Liu, L. Liu, C. Xu, L. Fu, Y. Wang, P.V. Nielsen, C. Zhang, Exploring the potentials of personalized ventilation in mitigating airborne infection risk for two closely ranged occupants with different risk assessment models, Energy Build. 253 (2021), https://doi.org/10.1016/j.enbuild.2021.111531.